Laminar Burning Velocities of Hydrogen and Ammonia Blends

Henriksen, M[a]., Shin, J[a,b]., Bjerketvedt D[a].
[a]University of South-Eastern Norway, Kjølnes Ring 56, Porsgrunn, 3901, Norway
[b]Norwegian University of Science and Technology, Trondheim NO-7491, Norway

1 Introduction

Ammonia is a promising carbon-free fuel due to its high energy density per volume compared to hydrogen. However, it faces challenges like toxicity, narrow flammability limits, and high ignition energy. Researchers are exploring blending ammonia with other fuels, such as hydrogen, to mitigate these issues and improve transportation efficiency. This blending can enhance fuel combustion properties, making it a viable solution for various applications. Laminar burning velocity (LBV) is a crucial combustion property that helps in understanding flame propagation, gas explosions, and combustion reaction mechanisms. It is also used in computational fluid dynamics (CFD) simulations to model turbulent combustion in large-scale explosions and safety engineering models. In this study, we have experimentally determined the laminar burning velocities for four different hydrogen-ammonia blends ([0.8:H2,0.2:NH_3], [0.6:H_2,0.4:NH_3], [0.5:H_2:0.5:NH_3], and [0.4:H_2:0.6:NH_3]) in air, at up to six different fuel-air equivalence ratios. In addition, the experimental results are compared to five different reaction mechanisms. To evaluate the prediction accuracy of the reaction mechanisms, the coefficient of determination (R^2) and standard deviation of the error (SDE) were calculated. To limit the scope, no sensitivity study on the chemical kinetics has been performed.

2 Materials and Methods

Figure 1 shows a schematic illustration of the experimental setup used in the study. Descriptions of the experimental setup, procedure, and determination of LBV have been published previously [1,2]. The internal volume of the explosion sphere is 20 L, and a temperature-controlled heating jacket surrounding the vessel regulates the inner ambient temperature. While two pressure sensors recorded the explosion pressure, a separate pressure sensor was used to record the ambient pressure in the vessel during filling. Moreover, the separated fuel and air inlets reduced uncertainties in fuel-air concentrations. A single high-voltage spark ignited the fuel-air mixture. The flame propagation was recorded using a high-speed camera operating at 20,000 frames per second (fps) and the shadowgraph imaging technique [30]. We analyzed each image using an in-house image-processing algorithm generated in Python (v3.6) to obtain the temporal evolution of the flame radius.

The planar unstretched laminar burning velocity (S_u^0) was calculated based on the temporal evolution of the flame radius. A detailed description of the procedure has been published previously [2,3]. The laminar flame speed (S_b^0) and the Markstein length (L_b) are curve-fitted to the implicit function of radii

($r(t)$) shown in Equation 1. From a previous study by Henriksen et al. [3], a comparison of the laminar burning velocity obtained by the most common stretch models showed that the models gave remarkably similar results. This study presents the laminar burning velocity obtained from the linear stretch model shown by Equations 1 and 2, which is commonly used in the literature.

$$r_f(t) = S_b^0 t - 2L_b \ln r_f + Cst \quad \text{Eq. 1}$$

where, r_f, flame radius [m], S_b^0, laminar flame speed relative to the burnt state [m s^{-1}], L_b, Markstein length relative to the burnt state [m], Cst, integration constant [m]

$$S_u^0 = S_b^0 \frac{\rho_b}{\rho_u}$$

where, S_u^0, laminar burning velocity relative to the unburnt state [m s^{-1}], S_b^0, laminar flame speed relative to the burnt state [m s^{-1}], ρ_b, density relative to the burnt state [kg m^{-3}], ρ_u, density relative to the unburnt state [kg m^{-3}].

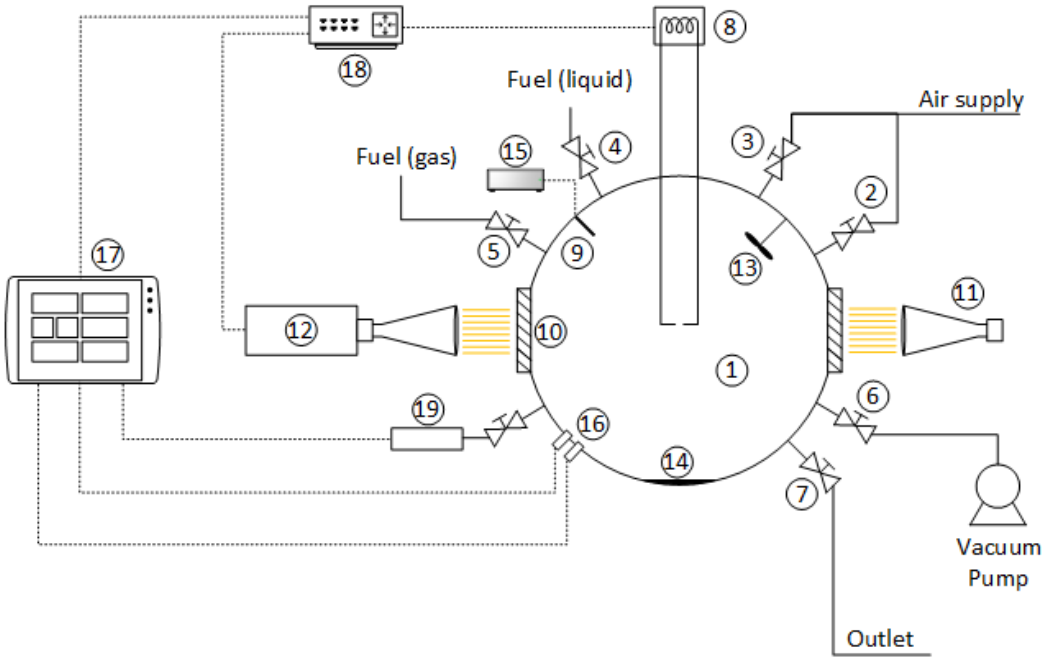

Figure 1: Schematic illustration of the experimental setup [1,2]. 1: explosion chamber; 2: oxidizer inlet; 3: flush inlet; 4: fuel (liquid) injection port; 5: fuel (gas) inlet; 6: vacuum port; 7: gas outlet; 8: ignition system; 9: thermocouple; 10: glass windows (100 mm); 11: LED light source; 12: high-speed camera; 13: stirrer; 14: heating plate; 15: ambient temperature display; 16: dual explosion pressure sensors; 17: data acquisition system; 18: control/trigger unit and 19: ambient pressure sensor

The numerical laminar burning velocities were calculated using the Python module Cantera [4], which comprises several routines and algorithms that aid in solving problems of thermodynamics, chemical kinetics, and transport processes. In this study, we used the *FreeFlame* algorithm that solves the governing equation of a steady laminar (planar) 1-D premixed adiabatic flame [5] to calculate the LBV. A chemical reaction mechanism is required to calculate the laminar burning velocity, which comprises the chemical kinetic, thermodynamic, and transport data of the included species and reactions. The results obtained from five different chemical kinetic models, namely, GRI-Mech 3.0 [6], Gotama et al. [7] (Gotama model), San Diego Mech [8], Otomo et al. [9] (Otomo model), and Zhu et al. [10] (Zhu model) were compared with the experimentally measured laminar burning velocity.

3 Results and Discussion

Several flame instabilities, such as thermal diffusion, hydrodynamic instabilities, and buoyancy, may influence flame propagation, generating uncertainties in the measured LBV [11]. To avoid instabilities due to buoyancy, only laminar burning velocities above 0.15 m/s were included, where the buoyancy effect can be neglected [12]. This criterion of 0.15 m/s also puts a constraint on the highest NH_3 ratio of 0.6 for this experimental setup.

As mentioned, the laminar flame speed and Markstein length are evaluated based on the record flame radius by Equation 1. Since the camera has a relatively high resolution of 0.081 mm per pixel, and the measured standard deviation of the radii and coefficients of determination are, on average, for all experiments 0.02 mm and 0.9999, respectively; Thus, the uncertainty in the regression coefficients, namely laminar flame speed (S_b^0) and Markstein Length (L_b), is negligible. However, this should not be mistaken for the uncertainty of S_b^0 and L_b, but only that the contribution to the uncertainty related to the curve fitting of the linear stretch model is relatively low.

Achieving smooth and spherical flame propagation, however, proved to be more challenging and could require many repeated experiments. Mainly, non-symmetrical ignition would occur, which caused the flame to propagate non-spherically. Furthermore, the increasing fraction of NH_3 increased the probability of ignition instabilities. It is worth noting that although experiments had non-spherical flame propagation, the measured laminar burning velocity was almost the same as a parallel experiment with proper flame propagation. Unfortunately, due to time constraints, this phenomenon cannot be investigated further. For a more comprehensive summary of the selection of experiments with acceptable flame propagation, the reader is referred to Jiyong Shin's Master thesis [13].

Table 1 summarizes the results for the four different hydrogen and ammonia mixtures. As expected, the mix with the highest laminar burning velocity is the mixture with the most hydrogen. The highest measured laminar burning velocity was 1.349 m/s and was found at an equivalence ratio of 1.4 for the mixture with 0.8 H_2 and 0.2 NH_3. However, the maximum laminar burning velocity for this mixture will be between an equivalence ratio of 1.2 and 1.4. For pure hydrogen, the laminar burning velocity is around an equivalence ratio of 1.65 [14]. The results in Table 1 show that the addition of ammonia into hydrogen shifts the maximum laminar burning velocities towards an equivalence ratio of 1.1, which is similar to most hydrocarbon fuels. Due to a relatively low energy high voltage spark generator, mixtures with a high ammonia concentration at fuel-rich conditions were unable to be ignited.

Table 1. Summary of the measured laminar burning velocities

Φ \ Fractions	**0.8 H_2 - 0.2 NH_3**	**0.6 H_2 - 0.4 NH_3**	**0.5 H_2 - 0.5 NH_3**	**0.4 H_2 - 0.6 NH_3**
0.8	0.94 m/s	0.50 m/s	0.33 m/s	0.23 m/s
1.0	1.21 m/s	0.63 m/s	0.43 m/s	0.29 m/s
1.2	1.35 m/s	0.65 m/s	0.43 m/s	0.29 m/s
1.4	1.35 m/s	0.51 m/s	0.31 m/s	0.24 m/s
1.8	1.00 m/s	0.33 m/s	No Ignition	No Ignition
2.0	0.84 m/s	N/A	No Ignition	No Ignition

Table 2 presents the coefficients of determination (R^2) and the standard deviation of the error (SDE) calculated from the experimental and numerical results from the five different reaction mechanisms. The GRI Mech 3.0 performs well when the hydrogen content in the mixture is high, which previous studies have also shown [1]. However, as the ammonia content increases, the deviation between experimental and numerical results increases significantly, as Table 2 and Figure 2 show. Of the five models, GRI Mech 3.0 has the lowest correlation and the highest SDE for the three mixtures that had an NH_3 fraction

of 0.4 or more of the five models. Since GRI Mech 3.0 is designed for natural gas combustion, it is not unexpected that it does not perform as well for gas mixtures with relatively high ammonia content.

Although the San Diego mechanism did not do as well as the three mechanisms that are more suited for H_2 and NH_3 combustion, it performed relatively consistently for all four mixtures. Although San Diego Mech had low R^2 values, its SDE was not as high as compared to the GRI Mech 3.0 at higher NH_3 fractions. Furthermore, the San Diego model had slightly lower R^2 values than the model by Otomo et al. for mixtures with an NH_3 fraction of 0.4 and higher; the San Diego model had almost the same or lower SDE values than the model by Otomo et al.

Table 2. The calculated coefficient of determination (R^2) and standard deviation of the error (SDE) for the five different reaction mechanisms.

Gotama et al.	**0.8 H_2 - 0.2 NH_3**	**0.6 H_2 - 0.4 NH_3**	**0.5 H_2 - 0.5 NH_3**	**0.4 H_2 - 0.6 NH_3**
R^2	0,814	0,957	0,961	0,862
SDE	0,119 m/s	0,033 m/s	0,015 m/s	0,021 m/s
Gri Mech 3.0	**0.8 H_2 - 0.2 NH_3**	**0.6 H_2 - 0.4 NH_3**	**0.5 H_2 - 0.5 NH_3**	**0.4 H_2 - 0.6 NH_3**
R^2	0,907	0,539	0,506	0,514
SDE	0,106 m/s	0,195 m/s	0,193 m/s	0,139 m/s
San Diego	**0.8 H_2 - 0.2 NH_3**	**0.6 H_2 - 0.4 NH_3**	**0.5 H_2 - 0.5 NH_3**	**0.4 H_2 - 0.6 NH_3**
R^2	0,774	0,746	0,645	0,681
SDE	0,151 m/s	0,084 m/s	0,066 m/s	0,045 m/s
Otomo et al.	**0.8 H_2 - 0.2 NH_3**	**0.6 H_2 - 0.4 NH_3**	**0.5 H_2 - 0.5 NH_3**	**0.4 H_2 - 0.6 NH_3**
R^2	0,920	0,849	0,653	0,549
SDE	0,083 m/s	0,079 m/s	0,083 m/s	0,089 m/s
Zhu et al	**0.8 H_2 - 0.2 NH_3**	**0.6 H_2 - 0.4 NH_3**	**0.5 H_2 - 0.5 NH_3**	**0.4 H_2 - 0.6 NH_3**
R^2	0,869	0,859	0,802	0,864
SDE	0,106 m/s	0,066 m/s	0,046 m/s	0,024 m/s

The three models proposed by Gotama et al., Otomo et al., and Zhu et al. were all designed for NH_3 and H_2/NH_3 oxidation; interestingly, however, there is a relatively large spread in the predicted laminar burning velocities. Of the three reaction mechanisms, the model from Gotama et al. and Zhu et al. had the least discrepancy with the experimental results. The model by Otomo et al. was in good agreement for mixtures with a low NH_3 content. However, as the fraction of NH_3 increased, so did the discrepancy with the experimental results, as shown in Figure 2 and by the decreasing R^2 in Table 2. The differences between the model from Gotama et al. and Zhu et al. were minimal, especially on the fuel-lean side.

Finally, evaluating and comparing chemical kinetic mechanisms can be much more compressive than in the done study. In this study, however, we only performed a statistical analysis that compared the experimental and numerical results and evaluated the accuracy of the laminar burning velocity prediction of these reaction models. The spread in measured laminar burning velocities between different experimental studies should be addressed. Moreover, the spread in laminar burning velocities in different experiments should be compared to the variation in the prediction accuracy of the various reaction mechanisms. However, this was beyond the scope of this study.

4 Conclusion

The study presented the investigation of the laminar burning velocities of hydrogen and ammonia blends, aiming for comparison with five chemical kinetics mechanisms. The laminar burning velocity was measured in a 20-liter explosion sphere at 300 Kelvin and 100 kPa. A total of four different H_2 and NH_3

gas mixtures were analyzed at different stoichiometries and compared to five different chemical kinetic models: GRI-Mech 3.0, Gotama et al., San Diego Mech, Otomo, et al., and Zhu et al.

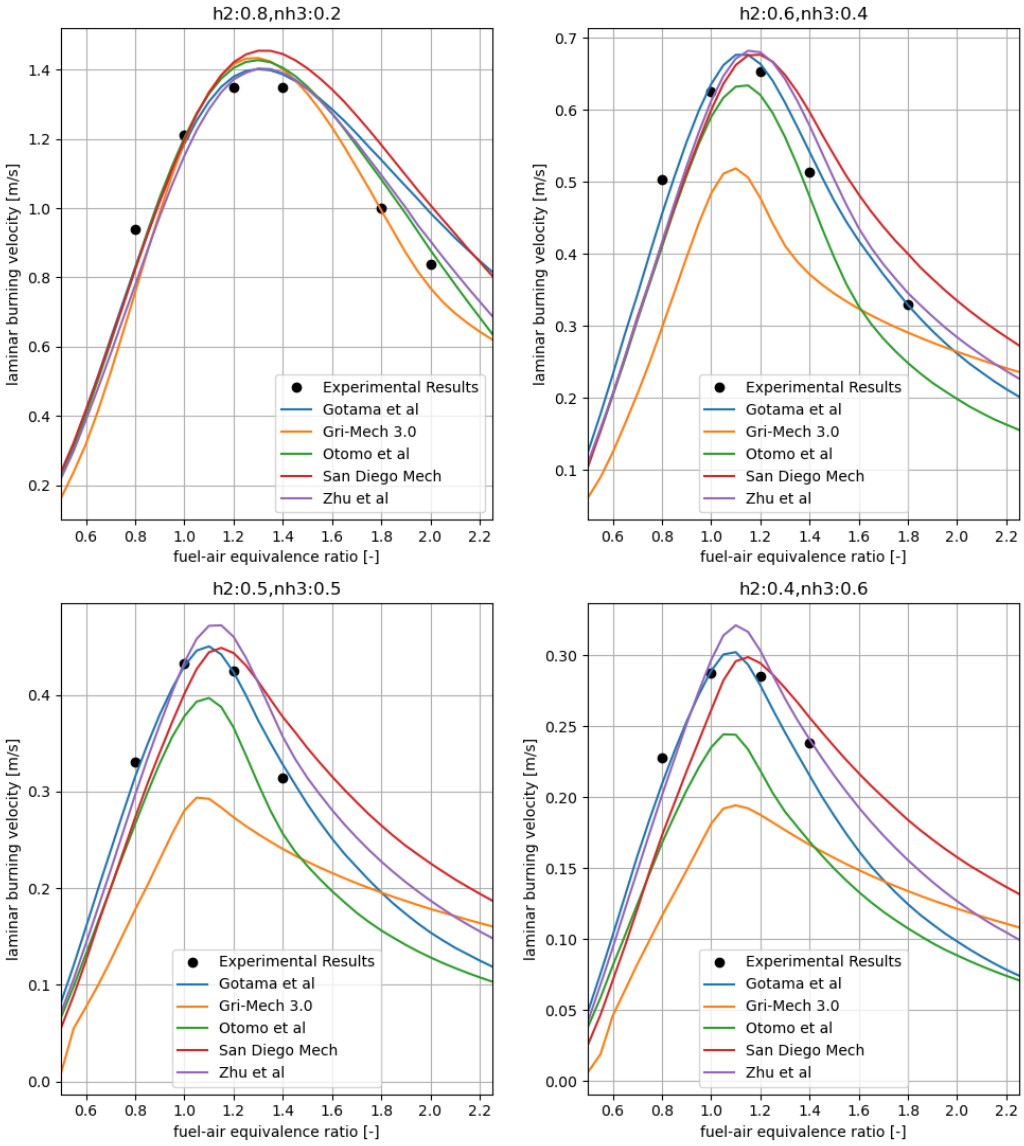

Figure 2. Comparison of the experimental and numerical results.

As expected, the results showed that the highest measured laminar burning velocity of 1.35 m/s at a fuel-air equivalence ratio of 1.4 was achieved with the mixture containing the most hydrogen. For this mixture, the maximum laminar burning velocity is between equivalence ratios of 1.2 and 1.4, while as the NH_3 content increases, the equivalence ratio goes towards 1.1. To achieve spherical flame propagation proved challenging, particularly with higher NH_3 concentrations. Although some experiments had non-spherical propagation, the measured laminar burning velocity did not differ much from an experiment with spherical combustion. Unfortunately, due to time constraints, this could not be investigated further.

The comparison of experimental and numerical results showed that the GRI-Mech 3.0 model performed well with high hydrogen content but deviated significantly with an increasing fraction of NH_3. The San Diego mechanism performed consistently across all mixtures, while the models by Gotama et al. and Zhu et al. showed the least discrepancy with experimental results. The Otomo et al. model performed well with low NH_3 content but showed increasing discrepancies with higher ammonia fractions.

References

[1] M. Henriksen, K. Vaagsaether, J. Lundberg, S. Forseth, D. Bjerketvedt, Laminar burning velocity of gases vented from failed Li-ion batteries, Journal of Power Sources 506 (2021) 230141. https://doi.org/10.1016/j.jpowsour.2021.230141.

[2] M. Henriksen, A study of premixed combustion of gas vented from failed Li-ion batteries, University of South-Eastern Norway, 2021. https://openarchive.usn.no/usn-xmlui/handle/11250/2829351.

[3] M. Henriksen, A.V. Gaathaug, K. Vaagsaether, J. Lundberg, S. Forseth, D. Bjerketvedt, Laminar Burning Velocity of the Dimethyl Carbonate-Air Mixture Formed by the Li-Ion Electrolyte Solvent, Combustion, Explosion, and Shock Waves 56 (2020) 383–393. https://doi.org/10.1134/S0010508220040024.

[4] D.G. Goodwin, H.K. Moffat, R.L. Speth, Cantera: An Object-Oriented Software Toolkit For Chemical Kinetics, Thermodynamics, And Transport Processes, (2017). https://doi.org/10.5281/zenodo.170284.

[5] J. Johnsplass, Lithium-ion battery safety, University of South-Eastern Norway, 2017.

[6] G.P. Smith, D.M. Golden, M. Frenklach, N.W. Moriarty, B. Eiteneer, M. Goldenberg, C.T. Bowman, R.K. Hanson, S. Song, W.C.G. Jr, V.V. Lissianski, Z. Qin, GRI-MECH 3.0, (1999). http://combustion.berkeley.edu/gri-mech/version30/text30.html#cite (accessed March 18, 2018).

[7] G.J. Gotama, A. Hayakawa, E.C. Okafor, R. Kanoshima, M. Hayashi, T. Kudo, H. Kobayashi, Measurement of the laminar burning velocity and kinetics study of the importance of the hydrogen recovery mechanism of ammonia/hydrogen/air premixed flames, Combustion and Flame 236 (2022) 111753. https://doi.org/10.1016/j.combustflame.2021.111753.

[8] UCSD, “Chemical-Kinetic Mechanisms for Combustion Applications”, San Diego Mechanism web page, Mechanical and Aerospace Engineering (Combustion Research), University of California at San Diego, The San Diego Mechanism (2016). http://combustion.ucsd.edu.

[9] J. Otomo, M. Koshi, T. Mitsumori, H. Iwasaki, K. Yamada, Chemical kinetic modeling of ammonia oxidation with improved reaction mechanism for ammonia/air and ammonia/hydrogen/air combustion, International Journal of Hydrogen Energy 43 (2018) 3004–3014. https://doi.org/10.1016/j.ijhydene.2017.12.066.

[10] Y. Zhu, H.J. Curran, S. Girhe, Y. Murakami, H. Pitsch, K. Senecal, L. Yang, C.-W. Zhou, The combustion chemistry of ammonia and ammonia/hydrogen mixtures: A comprehensive chemical kinetic modeling study, Combustion and Flame 260 (2024) 113239. https://doi.org/10.1016/j.combustflame.2023.113239.

[11] A.A. Konnov, A. Mohammad, V.R. Kishore, N.I. Kim, C. Prathap, S. Kumar, A comprehensive review of measurements and data analysis of laminar burning velocities for various fuel+air mixtures, Progress in Energy and Combustion Science 68 (2018) 197–267. https://doi.org/10.1016/j.pecs.2018.05.003.

[12] P.D. Ronney, H.Y. Wachman, Effect of gravity on laminar premixed gas combustion I: Flammability limits and burning velocities, Combustion and Flame 62 (1985) 107–119. https://doi.org/10.1016/0010-2180(85)90139-7.

[13] J. Shin, Hydrogen and ammonia combustion, Master Thesis, University of South-Eastern Norway, 2023.

[14] A.A. Konnov, Yet another kinetic mechanism for hydrogen combustion, Combustion and Flame 203 (2019) 14–22. https://doi.org/10.1016/j.combustflame.2019.01.032.

ACKNOWLEDGEMENT

This work was partially performed within HYDROGENI, a Norwegian Centre for Environment-friendly Energy Research (FME), co-sponsored by the Research Council of Norway (Grant No. 333118) and several partners from the research, industry, and public sectors.